Microchim Acta (2015) 182:2541–2549
DOI 10.1007/s00604-015-1625-2

ORIGINAL PAPER

Poly(*o*-phenylenediamine) nanosphere-conjugated capture antibody immobilized on a glassy carbon electrode for electrochemical immunoassay of carcinoembryonic antigen

Ti-Sen Xu[1] · Xiang-Yong Li[1] · Zhao-Hui Xie[1] · Xue-Gui Li[1] · Hai-Ying Zhang[1]

Received: 20 June 2015 / Accepted: 19 August 2015 / Published online: 1 September 2015

Abstract We report on a new electrochemical immunosensor for the carcinoembryonic antigen (CEA; a model analyte). First, poly(o-phenylenediamine) nanospheres (PPDNSs) were synthesized by using a wet-chemistry method. The nanospheres were utilized as the support for immobilizing horseradish peroxidase-labeled polyclonal rabbit anti-human CEA antibody (HRP-anti-CEA) on a pretreated glassy carbon electrode (GCE) using glutaraldehyde as a crosslinker. In the presence of target CEA, an antigen-antibody immunocomplex formed on the electrode. This results in a partial inhibition of the active center of HRP and decreases the activity of HRP in terms of H_2O_2 reduction. The performance and factors influencing the performance of the immunoelectrode were studied. Under optimal conditions, the reduction current obtained from the anti-CEA-conjugated HRP (best at a working voltage of −265 mV vs. Ag/AgCl) is proportional to the CEA concentration in the 0.01 to 60 ng mL^{-1} range, with a detection limit of 3.2 pg mL^{-1}. Non-specific adsorption was not observed. Relative standard deviations for intra-assay and inter-assay are <8.3 % and <9.7 %, respectively. The method was applied to the analysis of nine human serum samples, and a good relationship was found between the electrochemical immunoassay and the commercialized ELISA kit for human CEA.

✉ Ti-Sen Xu
tisenxu88@yeah.net

[1] Key Laboratory of Biotechnology and Biological Resource Utilization in Universities of Shandong, College of Life Science, Dezhou University, Dezhou 253023, Shandong, People's Republic of China

Keywords Electrochemical immunoassay · Differential pulse voltammetry · Cyclic voltammetry · Horseradish peroxidase · Poly(*o*-phenylenediamine) nanospheres · Nanoconjugation

Introduction

Carcinoembryonic antigen (CEA), as a set of highly related glycoproteins involved in cell adhesion, is normally produced in gastrointestinal tissue during fetal development, but the production stops before birth. However, the serum levels are raised in some types of cancers, e.g., liver, colon, breast and colorectal cancer [1]. Hence, the sensitive determination of CEA plays an important role in early monitoring and screening disease recurrence, contributing to tumor diagnosis and clinical therapy. Immunoassay, based on the antigen-antibody specific recognition interactions, has become the main analytical method to detect or quantify the tumor markers (which are found in the body, usually blood or urine) with high sensitivity and specificity [2, 3]. Various detection methods including fluoroimmunoassay, enzyme-linked immunosorbent assay (ELISA), electrochemical immunoassay, immunochromatographic assay, radioimmunoassay and chemiluminescence immunoassay, have already been reported for the determination of tumor markers [4–8]. Among these methods, the electrochemical immunoassay has attracted great attention because of its high sensitivity, simple instruments and low cost [9].

Electrochemical immunosensor studies the immunochemical reactions which take place in a solution at the interface of an electron conductor (a metal or a semiconductor) and an ionic conductor (the electrolyte), and which involve electron transfer between the electrode and the electrolyte or species in solution [10]. To develop the advanced electrochemical immunoassays, many works have been focused on using different nanomaterials for the

construction of the immunosensors, e.g., by noble nanostructures, organic-inorganic hybrid nanostructures and organic polymer nanomaterials [11]. Recent research has looked to develop innovative and powerful new nanomaterials, controlling and tailoring their properties in a very predictable manner to meet the needs of specific applications [12]. The power and scope of such nanomaterials can be heavily enhanced by coupling them with immunoreactions and electrical processes (e.g., nanobioelectronics). Poly(*o*-phenylenediamine) (PPD) is an interesting conducting polymer due to its high conductivity, electrochromic and photoelectronic properties with many free amino and imino groups [13]. Such PPD polymers naturally have both a pore size and a charged group that prevent interfering compounds from permeating them, so they have drawn wide interest in the fabrication of biosensors [14]. More significantly, the conducting PPD exhibits the strong electrochemical properties, which can be used as the mediator for the electron transfer [15]. In this work, our motivation is to synthesize the electroactive PPD nanostructures (PPDNS) for the construction of electrochemical immunosensor.

Using CEA as a model analyte, we design a new PPDNS-based immunosensing platform for the sensitive detection of CEA in the biological fluids. Initially, the positively charged PPDNS is immobilized onto the pretreated glassy carbon electrode with negative charges through the electrostatic reaction, and then horseradish peroxidase-labeled anti-CEA antibody is immobilized on the PPDNS by using glutaraldehyde as the cross-linkage reagent. Upon target CEA introduction, the formed immunocomplex on the electrode inhibited partially the active center of HRP, and decreased the immobilized HRP to H_2O_2 reduction. The electrochemical signal is registered through the labeled HRP toward catalytic reduction of H_2O_2 with the help of PPDNS. The reduction currents decreased with the increasing target CEA. By monitoring the change in the current, we can indirectly evaluate the concentration of target CEA in the sample. The aim of this work is to explore a new electroactive nanostructure-based immunosensing protocol for the detection of low-abundant protein without the participation of external electron mediator.

Experimental

Materials and reagents

Horseradish peroxidase-labeled polyclonal rabbit anti-human CEA antibody (HRP-*anti*-CEA) and CEA standards with various concentrations were purchased from Biocell Biotechnol. Co. Ltd. (Zhengzhou, China, www.chinabiocell.com). *o*-Phenylenediamine (OPD) (98 wt %), bovine serum albumin (BSA) and glutaraldehyde (25 wt %) were obtained from Sinopharm Chem. Re. Co., Ltd. (Shanghai, China, www.sinoreagent.com). All other reagents were of analytical grade and used without further purification. Double distilled water was used for all experiments. Phosphate buffer at various pH values were prepared by mixing the stock solutions of 0.1 M KH_2PO_4 and 0.1 M K_2HPO_4, and then adjusting the pH with 0.1 M KOH and H_3PO_4, and 0.1 M KCl was added as the supporting electrolyte. Clinical serum samples were gifted from Shandong Provincial Tumor Hospital, China.

Synthesis of poly(*o*-phenylenediamine) nanospheres (PPDNS)

Poly(*o*-phenylenediamine) nanospheres (designated as PPDNS) were synthesized through the redox processes of self-doped poly(*o*-phenylenediamine) in the presence of $K_2Cr_2O_7$ referring to the literature with minor modification [16]. Initially, 200 μL of 0.1 M OPD monomer was dispersed into 3 mL of distilled water. Then, 150 μL of 0.1 M $K_2Cr_2O_7$ aqueous solution was quickly added to the mixture. Afterwards, the mixture was stirred gently for 8 h at room temperature. The resulting suspension was centrifuged at 7000 g for 10 min. Finally, the obtained precipitate was re-dispersed into 1.0 mL of distilled water for further use.

Preparation of HRP-*anti*-CEA/PPDNS-functionalized immunosensor

A glassy carbon electrode (GCE, 3 mm in diameter) was sequentially polished with 0.3 and 0.05 μm alumina slurry, followed by successive sonication in distilled water, acetone, ethanol and distilled water for 2 min and dried in air. After that, a potential of + 1.75 V was applied to the electrode in 0.1 M pH 5.0 phosphate buffer for 300 s at room temperature. The electrode was then scanned between + 0.3 and + 1.3 V until a steady-state current-voltage curve was obtained [17]. After being washed with distilled water, 10 μL of PPDNS colloids (10 mg mL^{-1}) was dropped onto the resulting electrode, and incubated for 2 h at room temperature. During this process, the positive charged PPDNS was adsorbed to the negatively charged GCE via the electrostatic reaction. Following that, the modified electrode was incubated with the mixture containing 0.1 mg mL^{-1} HRP-*anti*-CEA and 1.0 wt % glutaraldehyde for 5 h at 4 °C under gentle shaking to yield HRP-*anti*-CEA/PPDNS-modified electrode. Finally, the immunosensor was incubated with 3.0 wt % BSA for 60 min at room temperature to eliminate non-specific binding effects and block the

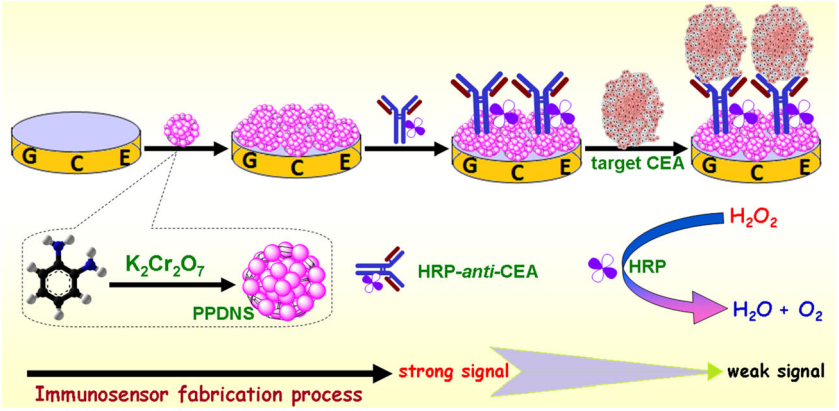

Scheme 1 Schematic illustration of poly(*o*-phenylenediamine) nanosphere (PPDNS)-functionalized immunosensor for one-step electrochemical detection of target CEA by using the PPDNS as indicator with enzymatic amplification

remaining active groups. The immunosensor was stored at 4 °C when not in use. The fabrication process of the immunosensor is illustrated in Scheme 1.

Immunoreaction protocol and electrochemical measurement

Voltammetric measurements were carried out with an AutoLab electrochemical workstation (μAUTIII.FRA2.v, Eco Chemie, The Netherlands, www.ecochemie.nl). A conventional three-electrode system used in the work consisted of a modified glassy carbon electrode as the working electrode, Pt wire as the counter electrode, and an Ag/AgCl reference electrode. Scheme 1 gives the fabrication process of the immunosensor and the assay principle of the electrochemical immunoassay. The assay was based on the inhibition of the activity of the immobilized HRP after the formation of the immunocomplex on the electrode. CEA standards or serum samples with various concentrations were initially prepared with distilled water, and then the immunosensor was incubated for 15 min with the samples at room temperature. After the residual was removed with doubly distilled water, the immunosensor was placed into pH 7.0 phosphate buffer containing 2.4 mM H_2O_2. Meanwhile, the signals were assayed by using differential pulse voltammetry (DPV) from −100 to −500 mV with a pulse amplitude of 50 mV and a pulse width of 50 ms. The DPV peak current was collected and registered as the signal of the immunosensor relative to CEA concentration (*Note*: All the currents were calculated relative to the base line throughout the text, unless specifically stated). The calibration plot was made by using the percentage decrease in the peak current relative to the background current [% = $(i_0 - i_n) \div i_0 \times 100$ %, where i_0 was the background current and i_n was the current toward different-concentration CEA]. All incubations and measurements were conducted at room temperature (25 ± 1.0 °C). All data were calculated in triplicate unless otherwise specifically stated.

Results and discussion

Characterization of the PPDNS

As mentioned above, the bioactivity of the immobilized biomolecules can be largely affected by the surface properties of the transducer during the preparation of the immunosensor. In this work, we tried to fabricate an improved sensing interface by using poly(*o*-phenylenediamine) nanospheres as the matrices. Use of nanospheres was expected to favor a particle-enhanced immobilization of biomolecules because of the unique physical and chemical features of nano materials. Figure 1a shows transmission electron microscopy (TEM, H600, Hitachi Instrument, Japan, www.hitachi.com) of the PPDNS, and the mean size was 30 nm. Such a structure provides a large surface coverage for the conjugation of biomolecules. Logically, an important concern arises to whether the PPDNS can be covalently conjugated to the pretreated GCE by the glutaraldehyde. To demonstrate this issue, we also used scanning electron microscopy (SEM, S-3400 N, Hitachi Instrument, Japan, www.hitachi.com) to monitor the pretreated GCE before and after conjugation with PPDNS and HRP-*anti*-CEA. Compared with the morphology of the pretreated GCE (Fig. 1b), we observed that many small-sized nanoparticles were coated on the surface of the pretreated GCE after incubation with PPDNS and HRP-*anti*-CEA (Fig. 1c). The results revealed that the PPDNS can be conjugated to the pretreated GCE by the glutaraldehyde.

Further, we also employed UV-vis absorption spectroscopy (Specord 250 plus, Germany, www.analytik-jena.com) to investigate the characteristics of *o*-phenylenediamine before and after the polymerization (Fig. 1d). As seen from curve '*a*', a strong characteristic peak at 290 nm was observed toward *o*-phenylenediamine alone, which was ascribed to the π-π* transition of the benzenoid rings [18]. After the formation of PPDNS, two new characteristic peaks at 259 and 420 nm were appeared, while the initial peak at 290 nm was disappeared (curve '*b*'). The phenomenon was in accordance with the previous reports [19, 20]. The peak at 259 nm derived from

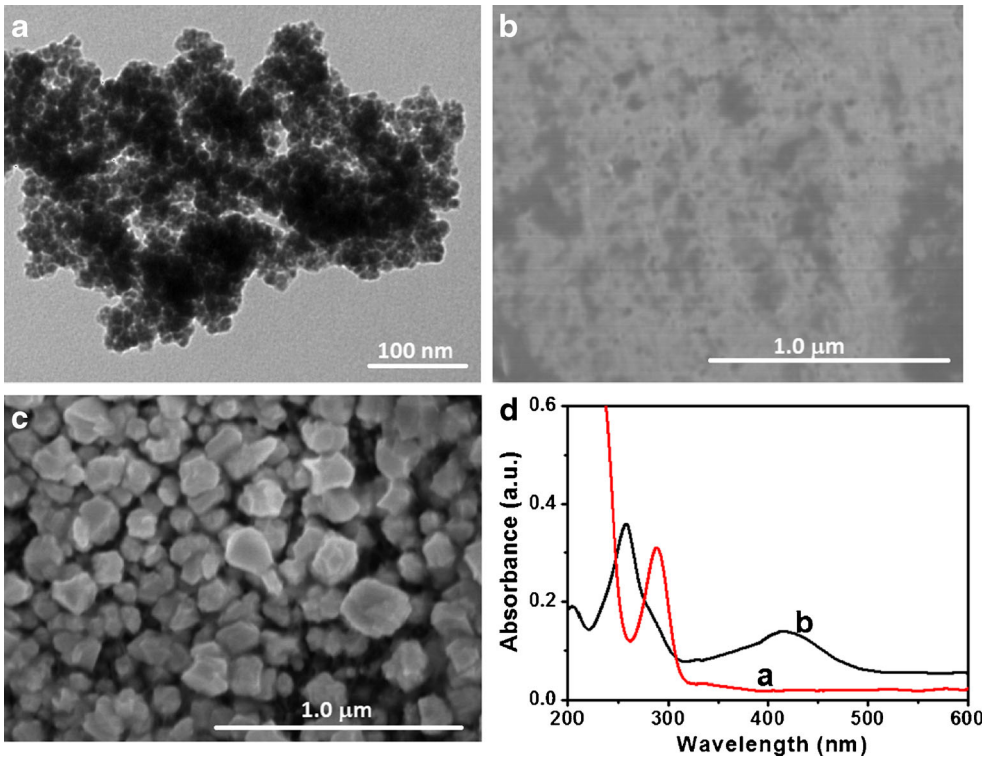

Fig. 1 **a** TEM image of the PPDNS, (**b**,**c**) SEM images of **b** the pretreated GCE and **c** PPDNS/HRP-*anti*-CEA-modified GCE, and **d** UV–vis absorption spectra of (**a**) *o*-phenylenediamine and (**b**) poly(*o*-phenylenediamine) nanospheres

the π-π* transition of the benzenoid rings. In contrast with *o*-phenylenediamine, the polymer displayed a distinct shift from 290 to 259 nm, which might be attributed to the formation of the C = N units, namely, quinoid units, a measure of oxidation state of the polymer [21, 22]. The characteristic peak at 420 nm originated from the charge transfer exciton-like transition about quinoid units [19, 22]. Thus, the successful preparation of poly(*o*-phenylenediamine) nanospheres favor for the construction of the immunosensor.

Electrochemical characteristics of variously modified electrodes

Figure 2a displays the cyclic voltammograms of the electrochemical immunosensor after each step in pH 7.0 phosphate buffer at 50 mV s^{-1}. No cyclic voltammetric peaks were observed at bare GCE (curve '*a*') and the pretreated GCE (curve '*b*') within the working potential range. In contrast with curve '*a*', the background current largely increased when the cleaned GCE was electrochemically pretreated (curve '*b*'). The reason might be attributed to the formation of –OH/–COOH groups on the electrode surface [17]. When PPDNS and HRP-*anti*-CEA were immobilized onto the resultant electrode, significantly, a couple of redox peak was achieved (curve '*c*'). The results indicated that the formation of poly(*o*-phenylenediamine) nanosphere did not change its redox properties, so that it can act as a mediator for electron communication between the solution and the base electrode. The redox reaction for poly(*o*-phenylenediamine) nanospheres can be illustrated as follows:

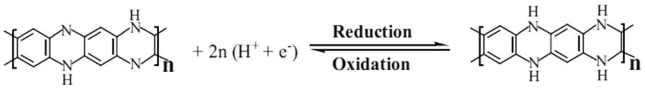

Typical cyclic voltammograms of the immunosensor in pH 7.0 phosphate buffer at different scan rates were studied (Fig. 2b). It was found that the the anodic and cathodic peak current increased with the increasing of scan rate where ΔE_p increased slowly. At the low scan rates, the peak current increased linearly with scan rate, *v*, not with $v^{1/2}$ (Fig. 2b, inset), suggesting that the redox reaction was a surface-controlled process. When $n\Delta E_p < 200$ mV, the electron transfer rate constant K_s of HRP on the immunosensor can be estimated by the following equation [23]:

$$\text{Log } K_s = \alpha\log(1-\alpha) + (1-\alpha)\log\alpha - \log(RT/nFv) - \alpha(1-\alpha)nF\Delta E_p/2.3RT$$

Taking a charge transfer coefficient α of 0.5, and a scan rate of 100 mV s^{-1}, and then the electron transfer rate constant (k_s) was 4.13 ± 0.64 s^{-1}, suggesting a reasonable fast electron transfer between the HRP and the electrode due to the presence of poly(*o*-phenylenediamine) nanospheres.

To further monitor the electrochemical characteristic of the immunosensor, H_2O_2 standards with different

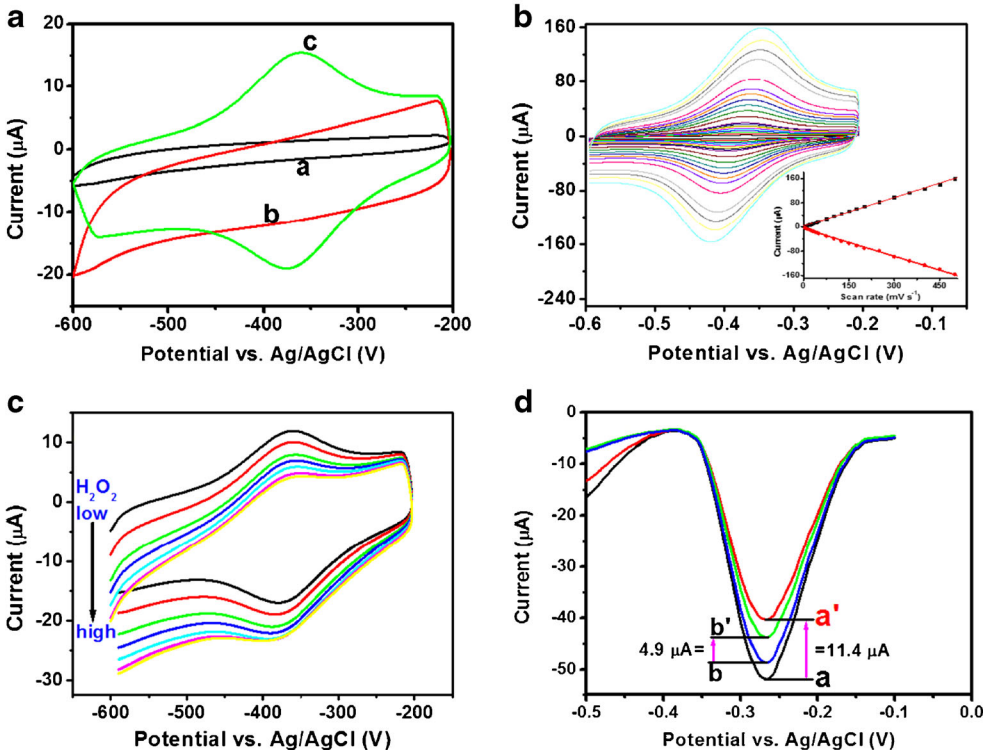

Fig. 2 **a** Cyclic voltammograms of **a** bare GCE, **b** the pretreated GCE and **c** HRP-*anti*-CEA/PPDNS -modified GCE in pH 7.0 phosphate buffer at 50 mV s^{-1}; **b** cyclic voltammograms obtained from HRP-*anti*-CEA/PPDNS-modified GCE at different scan rates (5–500 mV s^{-1} from inner trace to outer trace) in pH 7.0 phosphate buffer (*Inset*: plot of peak current against scan rate); **c** cyclic voltammograms obtained from HRP-*anti*-CEA/PPDNS-modified GCE in pH 7.0 phosphate buffer upon addition of different-concentration H_2O_2 from 0.01 mM to 2.0 mM; and **d** DPV responses of (**a,a'**) HRP-anti-CEA/PPDNS-modified GCE and (**b,b'**) anti-CEA/PPDNS-modified GCE in pH 7.0 phosphate buffer containing 2.4 mM H_2O_2 before (**a,b**) and after (**a',b'**) reaction with 1.0 ng mL^{-1} CEA

concentrations were added into 0.1 M phosphate buffer (pH 7.0), and cyclic voltammetric behaviors of the modified electrode was measured (Fig. 2c). As seen from Fig. 2c, upon the addition of H_2O_2 into phosphate buffer, an obvious catalytic characteristic was appeared with an increase of the cathodic current and a decrease of the anodic current. This result indicated the immobilized HRP in the electrode retains high enzymatic catalytic activity, and effectively shuttle electrons from the base electrode to the redox center of HRP. The electron transfer pathway can be simply summarized as follows:

$$\mathrm{HRP} + \mathrm{H_2O_2} \rightarrow \mathrm{Compound\ I} + \mathrm{H_2O}$$
$$\mathrm{Compound\ I} + \mathrm{PPDNS_{(red)}} \rightarrow \mathrm{Compound\ II} + \mathrm{PPDNS_{(ox)*}}$$
$$\mathrm{Compound\ II} + \mathrm{PPDNS_{(ox)*}} + 2\mathrm{H^+} \rightarrow \mathrm{HRP} + \mathrm{PPDNS_{(ox)}} + \mathrm{H_2O}$$
$$\mathrm{PPDNS_{(ox)}} + 2\mathrm{e^-} + 2\mathrm{H^+} \rightarrow \mathrm{PPDNS_{(red)}}$$

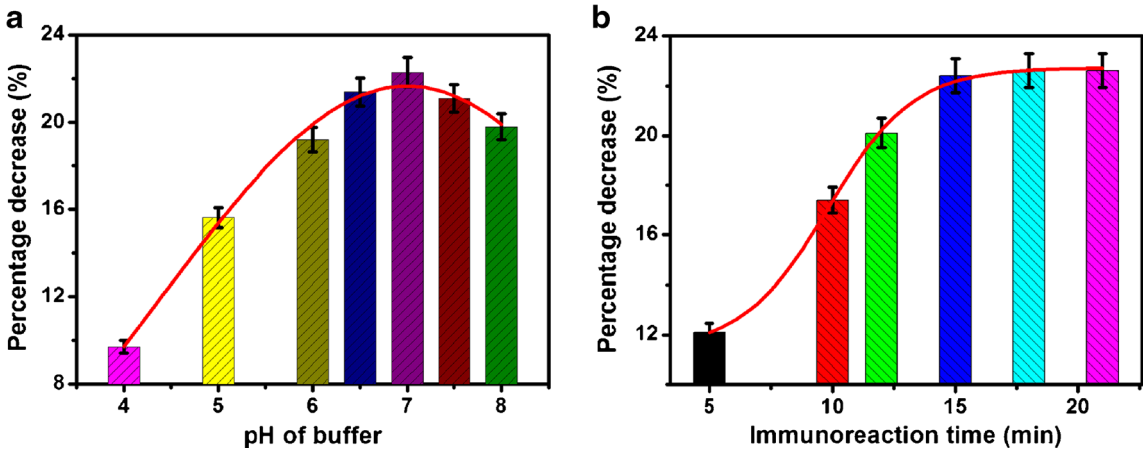

Fig. 3 The effects of **a** pH of phosphate buffer and **b** incubation time for the antigen-antibody reaction on the analytical properties of the electrochemical immunosensor (1.0 ng mL^{-1} CEA used in this case)

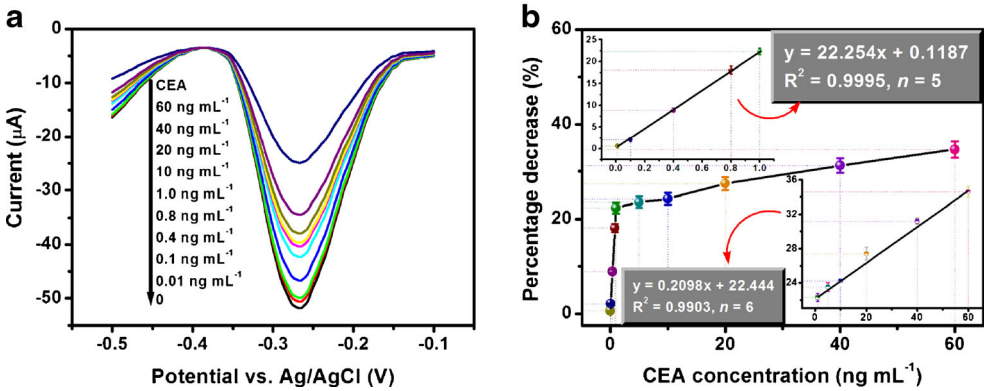

Fig. 4 **a** DPV responses of the electrochemical immunosensor toward different-concentration CEA standards in pH 7.0 phosphate buffer containing 2.4 mM H_2O_2, and **b** the corresponding calibration plots of the immunosensor (*Insets*: the corresponding linear curves at the low- and high-concentration range)

As described above, the PPDNS has a pair of redox peaks. After target CEA reacted with the immobilized HRP-*anti*-CEA, the formed immunocomplex coated on the modified electrode, and inhibited partly the active center of HRP and the redox efficiency of the PPDNS. Thus, the decreased electrochemical current was ascribed to the PPDNS and the immobilized HRP toward H_2O_2 reduction. The decrease in the reduction current indirectly depended on the CEA concentration in the sample.

To further clarify the advantage of using the HRP-anti-CEA, we prepared two types of immunosensors with and without the HRP by the similar preparation method (i.e., HRP-anti-CEA/PPDNS-modified GCE and anti-CEA/PPDNS-modified GCE). Following that, two immunosensors were used for the detection of 1.0 ng mL^{-1} CEA (as an example) in pH 7.0 phosphate buffer containing 2.4 mM H_2O_2. The comparison was evaluated on the basis of the change in the cathodic current before and after reaction with target CEA. As seen from Fig. 2d, the presence of HRP can cause an 11.4-μA signal decrease of the immunosensor, while the signal only decreased 4.9 μA without the HRP. So, use of HRP-anti-CEA had the ability to improve the analytical performance of the immunosensor.

Optimization of experimental conditions

To achieve an optimal analytical performance, some experimental parameters should be investigated. The influence of pH of phosphate buffer is an important parameter on the sensitivity of the electrochemical immunosensor, because the acidity of solution greatly affects the activity of the immobilized protein. Figure 3a shows the effect of pH of phosphate buffer on the current of the immunosensors in the buffer containing 2.4 mM H_2O_2 after incubation with 1.0 ng mL^{-1} CEA for 60 min (adequate reaction) at room temperature. The cathodic current increased with the increasing pH values from 5.0 to 7.0, and then decreased. The optimal amperometric response was achieved at pH 7.0. Highly acidic or alkaline surroundings would damage the immobilized protein, especially in alkalinity. So, pH 7.0 phosphate buffer was selected as the supporting electrolyte for CEA detection.

Usually, the antigen-antibody reaction is adequately carried out at human normal body temperature (37 °C). Considering the possible application of the proposed immunoassay in the future, we selected room temperature (25 ± 1.0 °C) for the antigen-antibody interaction throughout the experiment. At this condition, we monitored the effect of incubation time on the currents of the immunosensors from 5 to 30 min (Fig. 3b). As shown in Fig. 3b, the cathodic currents increased with the increment of incubation time, and tended to level off after 15 min. Hence, an incubation time of 15 min was selected for sensitive determination of CEA in this work.

Electrochemical responses of the immunosensors toward CEA standards

To enhance the probability for the effective treatment on the disease-relative proteins, highly sensitive detection of cancer markers is very important for early cancer diagnosis. Under the optimal conditions, the sensitivity and dynamic range of the electrochemical immunosensor were monitored toward CEA standards with the differential pulse voltammetry in pH 7.0 phosphate buffer containing 2.4 mM H_2O_2, using the PPDNS as the reporter. It was obvious that DPV peak currents displayed a dependence upon the concentration of target CEA (Fig. 4a), and the percentage decrease in the peak current increased linearly with the increasing of CEA concentration ranging from 0.01 to 60 ng mL^{-1} with two sections appeared. The linear regression equations were obtained as y (%) = 22.254 × $C_{[CEA]}$ (ng mL^{-1}) + 0.1187 (R^2 = 0.9995, n = 5) in the range of 0.01–1.0 ng mL^{-1}, and y (%) = 0.2098 × $C_{[CEA]}$ (ng mL^{-1}) + 22.444 (R^2 = 0.9903, n = 6) in the range of 1.0–60 ng mL^{-1} (Fig. 4b). The limit of detection (LOD) was 3.2 pg mL^{-1}, as calculated at the signal-to-noise ration of three. To further clarify the merits of the electrochemical immunosensor, the analytical properties were compared with other CEA immunosensing strategies (Table 1). Obviously, the LOD of PPDNS-based immunosensor was comparable with those of other CEA detection methods.

Table 1 Comparison of analytical properties of PPDNS-based electrochemical immunosensor with other CEA detection schemes existed

Detection method	Linear range	LOD	Assay time	Ref.
Amperometric immunoassay	0.01–100 ng mL^{-1}	4.2 pg mL^{-1}	>110 min	[24]
Amperometric immunosensor	0.01–100 ng mL^{-1}	2.7 pg mL^{-1}	>80 min	[25]
Amperometric immunoassay	0.01–100 ng mL^{-1}	8.6 pg mL^{-1}	>100 min	[26]
Surface plasmon resonance biosensor	1.0–60 ng mL^{-1}	1.0 ng mL^{-1}	~16 min	[27]
Electrochemiluminescent biosensor	0.001–80 ng mL^{-1}	0.3 pg mL^{-1}	>80 min	[28]
Impedimetric immunosensor	0.001–20 ng mL^{-1}	0.42 pg mL^{-1}	>140 min	[29]
Immunochromatographic test strip	–	2.0 ng mL^{-1}	15 min	[30]
Surface acoustic wave immunosensor	1.0–16 ng mL^{-1}	1.0 ng mL^{-1}	8 min	[31]
Human CEA ELISA kit: RAB0411	>0.343 ng mL^{-1}	0.15 ng mL^{-1}	>4 h	Sigma
Amperometric immunosensor	0.01–60 ng mL^{-1}	3.2 pg mL^{-1}	15 min	This work

Specificity and reproducibility and stability of the immunosensor

To validate the precision of determinations, we repeatedly detected 3 CEA standards with the identical batches of the immunosensors. Experimental results indicated that the relative standard deviations (RSDs) of the intra-assay were 8.3, 5.2 and 6.9 % for 0.1, 10, and 40 ng mL^{-1} CEA (n = 3), respectively, whereas the RSD of the inter-assay with various batches were 8.9, 9.7 and 8.3 % towards the above-mentioned levels. Hence, the precision and reproducibility of the electrochemical immunosensor were acceptable.

Next, the specificity of the electrochemical immunosensor was investigated by challenging the system against other biomakers, e.g., tissue peptide antigen (TPA), alpha-fetoprotein (AFP), cancer antigen 125 (CA 125), and prostate-specific antigen (PSA). As seen from Fig. 5a, the detectable signals of the immunosensor toward TPA, AFP, CA 125 and PSA alone were almost the same as the background signal, whilst the coexistence of interfering materials with target CEA did not cause the significant change in the signal compared with target CEA alone. Thus, the electrochemical immunosensor had a high selectivity toward target CEA.

When the immunosensor was not in use, it was dried and stored at 4 °C. No obvious change was observed after storage for 20 days, while the signal decreased ~90 % of initial signal on the 60th day. The slow decrease in the current might be attributed to the gradual deactivation of the immobilized HRP-*anti*-CEA on the electrode.

Analysis of real samples and method comparison

To investigate the feasibility of the immunosensor for the analysis of real samples, we collected nine human serum samples from Shandong Provincial Tumor Hospital, China. Prior to measurement, these specimens with high-concentration CEA were diluted to the linear range of the electrochemical immunosensor with blank human serum. Following that, these samples were monitored by using the electrochemical immunosensors based on the above-mentioned method. To evaluate the method accuracy, the assayed results were also compared with referenced values obtained from the commercialized human CEA ELISA kit (Fig. 5b). The comparison was performed by use of a least-squares regression between two methods: y = 1.0001 × + 0.1539 (R^2 = 0.9954, n = 9) (where x stands for CEA concentration estimated with the

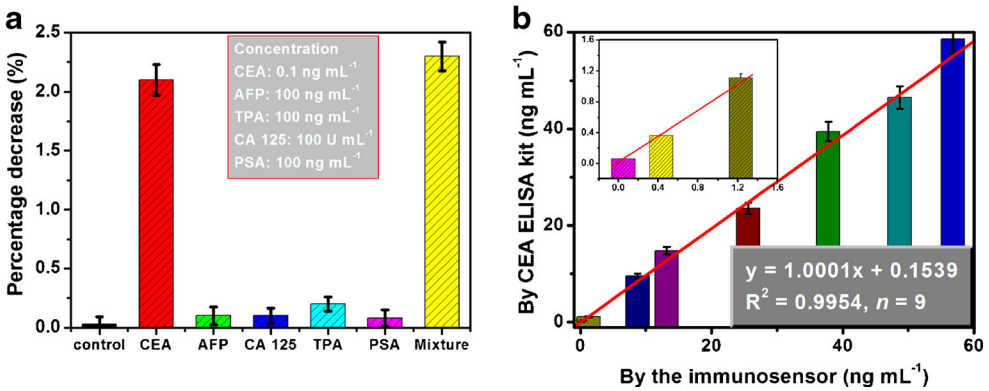

Fig. 5 **a** The specificity of the electrochemical immunosensor against CEA, TPA, AFP, CA 125, and PSA (*Note*: The mixture contained 0.1 ng mL^{-1} CEA, 100 ng mL^{-1} AFP, 100 U mL^{-1} CA 125, 100 ng mL^{-1} TPA and 100 ng mL^{-1} PSA), and **b** comparison of method accuracy for nine human serum samples between the electrochemical immunosensor and commercialized human CEA ELISA kit

electrochemical immunosensor and *y* stands for the referenced values). The slope and intercept of the regression equation were close to ideal values '1' and '0', respectively. Therefore, the electrochemical immunosensor can be used for the detection of CEA in biological fluids.

Conclusions

This work describes a sensitive and feasible electrochemical immunoassay for the carcinoembryonic antigen by using poly(*o*-phenylenediamine) nanospheres as the immobilization matrix. The assay was performed by using one-step immunoreaction between the immobilized antibody and analyte. Compared with conventional electrochemical immunoassays, our strategy can shorten the assay time and reduce the incubation steps, thus decreasing the assay cost. The system is capable of continuously carrying out all steps within below 20 min for one sample, including incubation, washing, enzymatic reaction and measurement, which is largely less than that of most commercialized ELISA kits (~3 h). Although the linear range is relatively narrow, it completely meets the requirement of clinical diagnostics since the threshold of CEA in human serum is 3.0 ng mL^{-1}.

Acknowledgments This work was financially supported by the Science and Technology Development Programs of Shandong Province of China (2013GSF11715).

References

1. Lin J, Zhang H, Niu S (2014) Simultaneous determination of carcinoembryonic antigen and α-fetoprotein using an ITO immunoelectrode modified with gold nanoparticles and mesoporous silica. Microchim Acta 182:719–726
2. Liu B, Zhang B, Chen G, Tang D (2014) Biotin-avidin-conjugated sulfide nanoclusters for simultaneous electrochemical immunoassay of tetracycline and chloramphenicol. Microchim Acta 181:257–262
3. Zhang K, Wu J, Li Y, Wu Y, Huang T, Tang D (2014) Hollow nanogold microspheres-signalized lateral flow immunodipstick for the sensitive determination of the neurotoxin brevetoxin B. Microchim Acta 181:1447–1454
4. Quesada-Gonzalez D, Merkoci A (2015) Nanoparticle-based lateral flow biosensors. *Biosens Bioelectron 73:47–63*
5. Chen A, Yang S (2015) Replacing antibodies with aptamers in lateral flow immunoassay. Biosens Bioelectron 71:230–242
6. Viswambari Devi R, Doble M, Verma R (2015) Nanomaterials for early detection of cancer biomarker with special emphasis on gold nanoparticles in immunassays/sensors. Biosens Bioelectron 68: 688–698
7. Creminon C, Taran F (2015) Enzyme immunoassays as screening tools for catalysts and reaction. Chem Commun 51:7996–8009
8. Rosenberg S, Restifo N (2015) Adoptive cell transfer as personalized immunotherapy for human cancer. Science 348:62–68
9. Zhang B, Liu B, Tang D, Niessner R, Chen G, Knopp D (2012) DNA-based hybridization chain reaction for amplified bioelectronic signal and ultrasensitive detection of proteins. Anal Chem 84:5392–5299
10. Pei X, Zhang B, Tang J, Liu B, Lai W, Tang D (2013) Sandwich-type immunosensors and immunoassays exploiting nanostructure labels: a review. Anal Chim Acta 758:1–18
11. Tang D, Cui Y, Chen G (2013) Nanoparticle-based immunoassays in the biomedical field. Analyst 138:981–990
12. Lin Y, Chen X, Lin Y, Zhou Q, Tang D (2015) Non-enzymatic sensing of hydrogen peroxide using a glassy carbon electrode modified with a nanocomposite made from carbon nanotubes and molybdenum disulfide. Microchim Acta 182:1803–1809
13. Salam S, Uzer A, Tekdemir Y, Erca E, Apak R (2015) Electrochemical sensor for nitroaromatic type energetic materials using gold nanoparticles/poly(o-phenylenediamine-aniline) film modified glassy carbon electrode. Talanta 139:181–188
14. Wang Z, Li X, Song Y, Li L, Shi W, Ma H (2015a) An upconversion luminescence nanoprobe for the ultrasensitive detection of hyaluronidase. Anal Chem 87:5816–1823
15. Li K, Guo D, Lin F, Wei Y, Liu W, Kong Y (2015a) Electrosorption of copper ions by poly(m-phenylenediamine)/reduced graphene oxide synthesized via a one-step in situ redox strategy. Electrochim Acta 166:47–53
16. Tian J, Li H, Luo Y, Wang L, Zhang Y, Sun X (2011) Poly(o-pheynylenediamine) colloid-quenched fluorescent oligonucleotide as a probe for fluorescence-enhanced nucleic acid detection. Langmuir 27:874–877
17. Wang H, Hu H, Chen, H (2001) Voltammetric behavior and detection of DNA at electrochemically pretreated glassy carbon electrode. Electroanalysis 13:1105–1109
18. Guo B, Finne-Wistrand A, Albertsson A (2011) Simple route to size-tunable degradable and electroactive nanoparticles from the self-assembly of conducting coil-rod-coil triblock copolymers. Chem Mater 23:1254–1262
19. Ding C, Li H, Hu K, Lin J (2010) Electrochemical immunoassay of hepatitis B surface antigen by the amplification of gold nanoparticles based on the nanoporous gold electrode. Talanta 80:1385–1391
20. Mani V, Chikkaveeraiah B, Patel V, Gutkind J, Rusling J (2009) Ultrasensitive immunosensor for cancer biomarker proteins using gold nanoparticle film electrodes and multienzyme-particle amplification. ACS Nano 3:585–594
21. Chen D, Feng H, Li J (2012) Graphene oxide: preparation, functionalization, and electrochemical applications. Chem Rev 112:6027–6053
22. Feng L, Chen Y, Ren J, Ou X (2011) A graphene functionalized electrochemical aptasensor for selective label-free detection of cancer cells. Biomaterials 32:2930–2937
23. Murray R (1984) In: Bard AJ (ed) Electroanalytical chemistry, vol 13. Marcel Dekker, New York, pp. 191–368
24. Chen H, Lai G, Fu L, Zhang H, Yu A (2015) Enzymatically catalytic deposition of gold nanoparticles by glucose oxidase-functionalized gold nanoprobe for ultrasensitive electrochemical immunoassay. Biosens Bioelectron 71:353–358
25. Xu T, Lin N, Yuan J, Ma Z (2015) Triple tumor markers assay based on carbon-gold nanocomposite. Biosens Bioelectron 70:161–166
26. Wang Z, Lin N, Feng F, Ma Z (2015b) Synthesis of cadmium, lead and copper alginate nanobeads as immunosensing probes for the detection of AFP, CEA and PSA. Biosens Bioelectron 70:98–105
27. Li R, Feng F, Chen Z, Bai Y, Guo F, Wu F, Zhou G (2015b) Sensitive detection of carcinoembryonic antigen using surface plasmon resonance biosensor with gold nanoparticles signal amplification. Talanta 140:143–149
28. Wang H, Yuan Y, Chai Y, Yuan R (2015c) Self-enhanced electrochemiluminescence immunosensor based on nanowires obtained by a green approach. Biosens Bioelectron 68:72–77

29. Hou L, Wu X, Chen G, Yang H, Lu M, Tang D (2015) HCR-stimulated formation of DNAzyme concatamers on gold nanoparticle for ultrasensitive impedimetric immunoassay. Biosen Bioelectron 68:487–493
30. Wang C, Hou F, Ma Y (2015d) Simultaneous quantitative detection multiplex tumor markers with a rapid and sensitive multicolor quantum dots based immunochromatographic test strip. Biosens Bioelectron 68:156–162
31. Zhang X, Zou Y, An C, Ying K, Chen X, Wang P (2015) Sensitive detection of carcinoembryonic antigen in exhaled breath condensate using surface acoustic wave immunosensor. Sens Actu B 217: 100–106